Optical spectroscopy of jet-cooled FeC between 12 000 and 18 100 cm^{-1}

Dale J. Brugh and Michael D. Morse[a)]
Department of Chemistry, University of Utah, Salt Lake City, Utah 84112

(Received 15 August 1997; accepted 8 September 1997)

Iron monocarbide has been investigated between 12 000 and 18 100 cm^{-1} in a supersonic expansion by resonant two-photon ionization spectroscopy. Six new electronic states have been identified for which origins relative to the ground state have been determined. Three of these possess $\Omega'=3$, one possesses $\Omega'=4$, and two possess $\Omega'=2$. The $\Omega'=3$ state with an origin near 13 168 cm^{-1} is likely a $^3\Delta_3$ state and has been assigned as the analog of the $[14.0]^2\Sigma^+\leftarrow X^2\Sigma^+$ charge transfer transition in CoC. The $\Omega'=4$ state is most likely a $^3\Phi_4$ state. Additionally, seven bands with $\Omega'=2$ have been observed that have proven impossible to systematically group by electronic state. Because every transition rotationally resolved in this study possesses a lower state with $\Omega=3$, the ground state has been confirmed as arising from an $\Omega=3$ state that is most likely the $\Omega=3$ spin orbit component of a $^3\Delta_i$ term derived from a $1\delta^3 9\sigma^1$ configuration. The ionization energy (IE) of FeC has been determined as 7.74 ± 0.09 eV by varying the wavelength of the ionization photon. When combined with the known IE of Fe and the bond energy of FeC^+, the bond energy of FeC is calculated to be 3.9 ± 0.3 eV. Presentation of the results is accompanied by an analysis of the bonding in FeC from a molecular orbital standpoint. © *1997 American Institute of Physics.* [S0021-9606(97)02746-3]

I. INTRODUCTION

Progress in characterizing the transition metal–carbon bond in the simplest of systems, the metal monocarbides, by high resolution spectroscopic methods can be divided roughly into two time periods. First was the work done by Scullman *et al.* on PtC,[1] RhC,[2] IrC,[3] and RuC[4] prior to 1980. These detailed investigations provided the only understanding of the bonding in such molecules for a number of years, but these studies had their problems. Because the metal carbide was produced at high temperature in a furnace, necessitated by the refractory nature of both the metal and carbon, it was sometimes not possible, as in the case of RuC, to observe the first lines in the rotationally resolved spectrum and thereby identify the electronic states involved. The electronic and geometric structure of these species, however, is crucial to understanding such molecules and in building a base for understanding larger systems that include metal–carbon bonds. Such systems appear quite often in industry and in systems of biological importance. The central role of iron in our own species' biology is just one example. In addition, more exotic environments such as stellar atmospheres cannot be fully understood until all the chemical participants and their abundance can be identified, but work in identifying potentially important constituents, such as some metal carbides, is hampered by the lack of laboratory data.

The development and maturation of laser vaporization/supersonic expansion techniques for the ready production of refractory species in the gas phase ushered in a new era of study of the metal–carbon bond that was begun by Simard, Hackett, and Balfour[5] with a report in 1994 of the spectrum of YC. With the completion of this investigation, it was clear that future work on transition metal carbides would be interesting because YC did not have the ground state that would be predicted based upon the orbital energy ordering of the early oxides.[6] In part, this was expected because of the better match between the energies of the $2s$ and $2p$ orbitals of C with those of the metal than in the case of the oxides, but even the calculations by Shim, Pelino, and Gingerich[7] failed to provide conclusive evidence of what the ground state of YC would be. For YC, the ground state is now known to be $^4\Pi$ deriving from a $10\sigma^2 11\sigma^1 12\sigma^1 5\pi^3$ configuration. One investigation, however, does not impart an immediate understanding of the subtleties of the bonding across the transition series. Following the work of Simard, of course, the number of carbides investigated for the first time in the gas phase or reinvestigated has increased dramatically, and the possibility for a systematic investigation of transition metal carbides now exists.

It is not the purpose of this article to review all the current work on transition metal carbides. The focus here is on the $3d$ metal carbides and FeC in particular. Iron monocarbide was the first of the $3d$ carbides to be investigated in the gas phase by electronic spectroscopy.[8] Soon thereafter, the spectrum of CoC was reported by Barnes, Merer, and Metha,[9] which was later supplemented by the work of Adam and Peers[10] on an additional band system. These constitute the only published gas phase electronic spectroscopic studies of the $3d$ transition metal monocarbides, although unpublished studies of TiC, VC, CrC, and NiC exist.[11] In a continuing effort to better understand the bonding in all the carbides, we have investigated the spectrum of FeC further to the red of the original study by Balfour. The work presented here is an incremental improvement in the understanding of the nature of the iron to carbon bond in FeC. Several new electronic states have been identified, but complexities that are common to many transition metal carbide optical spectra

a)Electronic mail: morse@chemistry.chem.utah.edu

are also present here. For example, a number of the rotationally resolved bands in this study cannot be grouped according to electronic states, and perturbations are evident throughout the spectrum. This article is also the first of five articles from this group covering work on the transition metal monocarbides. The remaining four articles will discuss results for RuC, PdC, NiC, and MoC.

II. EXPERIMENT

A. Overview

The apparatus used in the present study of FeC is a two stage differentially pumped vacuum system consisting of a source chamber and a time-of-flight mass spectrometer (TOFMS). It is essentially the same as that used to interrogate numerous other molecules in this group. A scale drawing can be found with our original work on aluminum trimer.[12] In general, the molecules of interest are generated in the throat of a supersonic expansion by the pulsed laser ablation of a metal target disk that is both rotated and translated to evenly remove metal from the disk surface.[13,14] The supersonically cooled molecular beam is skimmed (Beam Dynamics, 5 mm diam, 50° inside angle) and allowed to enter the extraction region of a reflectron TOFMS where spectroscopy is performed.

The most common method used to carry out a spectroscopic investigation of a particular species in the molecular beam that has entered the TOFMS is to expose the beam to the output of a tunable laser directed along the propagation axis of the expansion and to cross that with the output of an excimer laser about 20 ns later in time. The dominant photoionization processes in the TOFMS under this experimental setup are direct one-photon ionization, most commonly induced by the excimer laser; nonresonant two-photon ionization, again, most commonly induced by the excimer; and resonant two-photon ionization (R2PI), which is induced by the resonant absorption of one photon of the tunable laser followed by one of the excimer laser output. To conduct a systematic study of a particular species in the molecular beam, the direct one-photon ionization of the molecule of interest must be eliminated, the nonresonant two-photon signal must be minimized, and the tunable laser source must be scanned to produce ions of the neutral species of interest by R2PI.

The ions produced in each experimental cycle are separated by mass and detected by a microchannel plate assembly (Galileo, model 3025-B) coupled to a 50 Ω anode assembly. The signal is amplified (Pacific Instruments, model 2A50) and digitized by a 100 MHz transient digitizer (Transiac, model 2001). The digital signal representing the mass spectrum of the ions is signal averaged, displayed, and stored in real time by a 40 MHz 386-SX PC clone based computer system at a repetition rate of 10 Hz. The timing of all pulsed devices (nozzle, three Q-switched Nd:YAG lasers, and one excimer) and all triggerable devices (digitizers and gated integrators) is achieved with a temporal resolution of 200 ns by the use of three delay generating chips (Advanced Micro Devices, model Am9513A) interfaced directly to the PC bus via two cards built in the University of Utah Chemistry Department Electronics Shop (Peaceable I Multifunction Cards). A better timing resolution of 1 ns can be achieved with a different delay generator (Evans Electronics, model 4141) when the delay between two lasers must be controlled to within the jitter of the lasers (2 ns). Ancillary data such as relative laser fluence, étalon transmission fringes, and iodine absorption or fluorescence is averaged, displayed, and stored by the same computer by first integrating the corresponding photodiode or photomultiplier signal with a home built integrator and then digitizing that signal with a set of analog to digital convertors (Analog Devices, AD578J) located on the multifunction cards attached to the PC bus.

B. Molecular sources

In this study, the most efficient production of FeC was accomplished by the pulsed laser ablation of a carbon steel target disk with 1 to 2 mJ of the second harmonic output from a Nd:YAG laser in the throat of a supersonic expansion of 3% methane in helium that was allowed to expand through a 2 mm orifice after traveling through a 3 cm channel. The gas plenum was maintained at a pressure of between 60 and 80 psig for all work. This has become a common technique for generating carbon-containing molecules from refractory metals.[8,15] A number of other molecular production methods were tried, but all were less successful. The substitution of ethylene for methane in the helium carrier gas resulted in no observable FeC ion enhancement while the substitution of acetylene resulted in a two-thirds drop in the production efficiency of iron carbide. The mole percent of carbon in the carbon steel sample disk was too low to allow the production of an observable number of FeC molecules in a pure helium expansion. The substitution of a powder pressed sample disk consisting of iron and carbon powders in the mole ratio 3:1 was found to be about half as efficient at producing FeC as the helium/methane/carbon steel production route. It was this last technique which afforded us our first observation of resonant enhancement in FeC, but it was not subsequently employed. For vaporization of the metal target, the second harmonic output (532 nm) of one of three Nd:YAG lasers (Quantel model 580-10; Quantel model 581-C, Continuum Powerlite 8000) was focused to a spot size of 0.5 mm on the sample disk. The choice of vaporization laser was purely a matter of convenience and resulted in no essential difference in the observed signal. All data presented here were collected under the most efficient production conditions for FeC.

C. Spectroscopy sources

The excitation photon for the R2PI process was supplied by either of two possible sources. The first source was the output of a refurbished Molectron dye laser (Molectron DL-222) pumped by the frequency doubled output of a Nd:YAG laser (Quantel model 581-C). This laser provided low resolution laser radiation ($0.6\ \mathrm{cm}^{-1}$) at high pulse energy (10–50 mJ), tunable over a wide spectral region ($12\,000–18\,200\ \mathrm{cm}^{-1}$), using a variety of dyes for use in

survey scans of FeC. To conduct low resolution scans from 12 000 cm^{-1} down to the limit of this study at 10 400 cm^{-1}, we placed a steel tube filled with H_2 at 500 psig in the path of the focused dye light. This allowed us to generate the first Stokes radiation via stimulated Raman scattering off the $Q(1)$ line of H_2. As described by Clouthier and Karolczak,[16] this provided laser radiation of comparable linewidth to the input radiation but shifted 4155.162 cm^{-1} to the red.

This laser source also produced higher resolution radiation (0.04 cm^{-1}) at lower energy (1–5 mJ) over a much narrower spectral window ($\sim$15 cm^{-1}) for use in resolving the rotational structure of many of the bands observed in the low resolution spectrum. Achieving the higher resolution was accomplished by the insertion of an air spaced étalon (Lambda Physik) into the oscillator cavity of the dye laser. The cavity was then evacuated and pressurized (Molectron DL-224) back to 650 Torr with Freon 12 (CCl_2F_2, DuPont) at a rate of about 8 Torr/min. All but one of the 22 rotationally resolved bands in this study were resolved with this source in high resolution mode.

The second source in this study was the output of a Continuum Mirage 500 optical parametric oscillator (OPO)/optical parametric amplifier (OPA) combination. In this package, the OPO was pumped by approximately 20 mJ of the nearly gaussian second harmonic light of an injection seeded Nd:YAG laser (Continuum Powerlite 8000). The parametric conversion process in the oscillator's KTP crystal generated two photons of lower frequency, one of which was selected to seed the amplifier's two BBO crystals. At the same time that the seed photon from the oscillator entered the BBO crystals, approximately 150 mJ of the third harmonic radiation from the same YAG laser was directed through the amplifier. The seed photon was amplified to yield about 10 mJ of high resolution laser radiation (0.02 cm^{-1}). As a consequence of the conservation of energy, a second photon was also produced in the amplifier of frequency $\omega_{pump}-\omega_{seed}$. Both had the same linewidth. The two wavelengths were separated by a set of dichroics that were supplemented with prisms and filters to insure that only the desired wavelength was transmitted. This package was used to rotationally resolve one band in this study.

D. Ionization sources and lifetime collection

The second photon, the ionization photon, was supplied by the output of an excimer laser (Lambda Physik, Compex 200) operating on an ArF gas fill at 193 nm (6.42 eV, 50–80 mJ/pulse). This ionization source was used for all survey and high resolution work. To determine the ionization energy of the molecule, the excimer laser was fitted with unstable resonator optics to decrease the divergence of the output beam, and the beam (200 mJ) was then focused through a high pressure cell of H_2 (310 psig) to generate Raman-shifted radiation. The cell construction has been described in detail previously.[17] The output beam of the Raman shifter was heavily filtered with salt plates (NaCl) and a 193 nm 45° reflector (Acton Research) to eliminate any trace of the original ArF pump light. The fused silica windows used in the Raman shifter (Corning 7940-UV) eliminated any anti-Stokes radiation that may have been generated. Less than 1 mJ of the first Stokes light (5.90 eV, 210 nm) remained for ionization. It was, however, sufficient to conduct experiments.

Lifetimes of excited electronic states were determined by the time delay technique in which the FeC^+ signal intensity is collected as a function of the delay between the excitation and ionization photons when the excitation laser is tuned to a resonant transition. At near temporal coincidence of the two photons, the ion signal is the greatest. It decays exponentially as the delay is increased. This decay is then fit to one of six different exponential decay models using a nonlinear least squares fitting routine.[18] Four of the six models available for fitting these decays include a convolution of the excitation and ionization laser profiles into the exponential decay to better describe curves obtained for electronic states with short lifetimes ($<$200 ns).

E. Calibration techniques

Absolute frequency calibration of the rotationally resolved bands of FeC was accomplished by simultaneously collecting the spectrum of I_2, the spectrum of the molecule of interest, and the étalon transmission fringes with the same high resolution dye laser radiation. The iodine spectrum was then compared to either the atlas of Gerstenkorn and Luc[19] or the atlas of Gerstenkorn, Verges, and Chevillard[20] to find an exact match. By plotting the absolute frequencies from the iodine atlas as a function of fringe number and fitting this to a straight line, it was possible to determine the free spectral range of our étalon, necessary for properly determining the relative position of the lines in the molecular spectrum, and the shift to apply to our spectrum, necessary to obtain absolute wavenumber positions for each line. The spectrum of iodine was collected by fluorescence (15 300 – 20 000 cm^{-1}), direct absorption of I_2 at 25 °C (15 000–15 300 cm^{-1}), direct absorption of I_2 at 250 °C (14 000–15 000 cm^{-1}), or direct absorption of I_2 at 500 °C (12 900–14 000 cm^{-1}). The iodine cell was heated by means of a quad-elliptical radiant heater supplied by R. I. Controls (Model E4-10). Following a correction for the Doppler shift due to the motion of the molecules toward the excitation radiation and a correction for the error in the first atlas mentioned above,[21] the reported line positions are believed to have an accuracy of $\pm$0.005 cm^{-1}.

In the case of the one band at 12 000 cm^{-1} that was rotationally resolved with the Mirage 500, it was not possible to calibrate with the same laser radiation used to excite the molecule because we lacked the ability to heat the iodine to 790 °C. Instead, we were able to use to our advantage the fact mentioned in Sec. II C that the Mirage 500 simultaneously outputs two tunable laser beams of different frequency and of comparable quality. The sum of the frequencies of the two output photons must always equal the frequency of the third harmonic light (3ω) of the Nd:YAG laser used to pump the OPA. By collecting the molecular spectrum of FeC with one output of the Mirage 500 (ω_{FeC})

near 12 000 cm^{-1} and the iodine fluorescence spectrum of the other output (ω_{iodine}) near 16 000 cm^{-1} simultaneously, it was only necessary to know the value of 3ω to absolutely calibrate the molecular spectrum by the difference $\omega_{FeC}=\omega_{pump}-\omega_{iodine}$. We were able to find a spectral region in which one output of the Mirage 500 could be calibrated by fluorescence in one atlas while the other output could be simultaneously calibrated in the other by absorption at 500 °C. Using this technique, we were able to determine the sum of the frequencies of the two Mirage 500 output photons, and thus the ω_{pump} of the pump YAG was determined to be $28\,183.4182\pm0.0002$ cm^{-1}. It was then possible to collect a molecular spectrum of FeC with the lower energy output of the OPO/OPA near 12 000 cm^{-1} while simultaneously collecting the iodine fluorescence due to the higher energy output near 16 000 cm^{-1} and absolutely determine the line positions of FeC. We call this calibration technique OPO/OPA differential calibration. Clearly, the calibration of the pump YAG 3ω must be performed routinely if OPO/OPA differential calibration is to be used to reliably determine absolute line positions.

III. RESULTS

This spectroscopic study of iron monocarbide was conducted from 10 400 to 18 100 cm^{-1}. Below 12 000 cm^{-1}, however, it was not possible to probe and detect resonant excitation because the photons provided by the ionization laser were not sufficiently energetic to ionize states that might be present in that region. This is discussed in more detail in Sec. III H. Between 12 000 and 18 100 cm^{-1}, at least 44 bands have been observed, making this spectrum nearly as dense as that observed by Balfour[8] between 20 000 and 23 256 cm^{-1}. Of the 44 bands, 22 were selected for study at higher resolution to reveal the rotational structure of each. The analysis of these bands has yielded a general picture of the excited electronic state manifold in this region. It is clear that FeC possess three excited states with $\Omega=3$ symmetry, two of which have their band origins near 13 200 cm^{-1}. The remaining $\Omega=3$ state has an origin near 15 450 cm^{-1}. These three states account for 8 of the 22 resolved bands. Also near 13 100 cm^{-1} is the origin of a state with $\Omega=4$ symmetry that displays a three band progression. Diatomic FeC also possess at least three states of $\Omega=2$ symmetry. One of these has an origin at 12 000 cm^{-1}, and another has an origin near 16 000 cm^{-1} with a three band progression. The 1-0 band of the state with an origin near 12 000 cm^{-1} may also be observed, but it was not rotationally resolved. The remaining seven bands all possess $\Omega=2$, but it is not clear which of these belong together as members of a progression. All of the bands possess $\Omega''=3$. In the sections that follow, each of these band systems will be described, and the determination of the ionization energy of FeC will be discussed. If more detailed information about any of the rotationally resolved bands is desired, a complete list of line positions can be obtained from the Physics Auxiliary Publication Service (PAPS) of the American Institute of Physics or from the author (M.D.M.).[22]

A. General fitting procedure

The initial study of every rotationally resolved band in FeC proceeded by first fitting the observed rotational structure to the standard formula

$$\nu=\nu_0+B'_v J'(J'+1)-B''_v J''(J''+1). \tag{3.1}$$

This allowed lower and upper state rotational constants to be extracted, which aided in the assignment of vibrational progressions and in the choice of new bands for rotational analysis. No account was taken of centrifugal distortion because, initially, it was assumed to be small at the low J observed. No evidence was found for lambda doubling; consequently, this effect was ignored. As expected, the B''_0 values determined in this way were not identical because the quality of the data for each band was not identical. The weighted average of all the values, however, was found to be 0.669 567(21) cm^{-1}. Late in 1996, Allen and co-workers[23] reported the observation of six pure rotational transitions within the $\Omega=3$ ground state of FeC. This allowed the determination of the ground state rotational constant for FeC with, by optical standards, extreme precision. Their value for B''_0 was determined to be 0.669 643 18(7) cm^{-1}, where the 1σ error limit is in parentheses. Though very close to the weighted average value of B''_0 determined in this study, it was decided that the value from Allen *et al.* was simply more accurate and should be accepted as correct. Every band in this study was then refit holding the value of B''_0 fixed to this value. This is why no lower state rotational constants are reported in this study. The value of B''_0 was always fixed to 0.669 643 18 cm^{-1} for $^{56}Fe^{12}C$ and 0.674 144 02 cm^{-1} for $^{54}Fe^{12}C$.

The study by Allen *et al.* also determined that the centrifugal distortion constant in the ground $\Omega=3$ state is a mere 1.6142×10^{-6} cm^{-1}, a value that would not lead to noticeable effects even at the highest J observed in our bands. Even in the refit of all bands in this study to hold B'' fixed the effects of centrifugal distortion were not considered.

B. The FeC [13.17]$\Omega=3\leftarrow X\,^3\Delta_3$ system

This band system consists of six observed bands ranging from 14 600 cm^{-1} to the limit of this study at 18 100 cm^{-1}. The bands are weak and have long lifetimes that average 5.8 μs. It was possible to rotationally resolve the major isotope, $^{56}Fe^{12}C$, for each of these bands, but the same could not be done for the minor isotope $^{54}Fe^{12}C$. This precluded the determination of precise isotope shifts. It was possible, however, to determine the isotope shift for each of these bands by finding the separation between the R-band heads for each isotope. This allowed the shifts to be determined with about a one half wavenumber uncertainty. The appearance of the rotational structure of each of these bands is illustrated by that of the highest member of this progression shown in Fig. 1. The immediate band head in the R branch is a clear indication that the bond length increases dramatically upon ex-

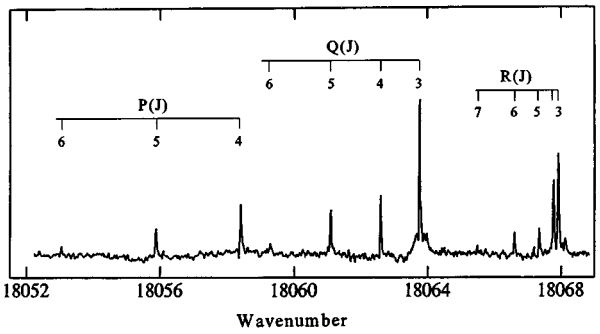

FIG. 1. Rotationally resolved spectrum of the 7-0 band of the $[13.17]\Omega=3$ system. The immediate band head in the R branch, due to a large increase in bond length upon excitation, causes all branches to fan out to lower energy. The first line in each branch is clearly distinguishable, and the assignment of the first lines identifies the transition as $\Omega=3\leftarrow\Omega=3$.

citation. The relevant data for this band system and for all other bands rotationally resolved in this study is summarized in Table I.

As can be seen in this table, the observed isotope shift for the first band in this progression at $14\,608\ \mathrm{cm}^{-1}$ $(+4.45\ \mathrm{cm}^{-1})$ is much too large for an origin band. Each band does appear, however, to originate from the $v=0$ level of the ground state based upon the value of B'' obtained for each band prior to holding B'' fixed. In order to determine an absolute vibrational numbering for this system, several different vibrational numbering schemes were tried. The band origins were fit with each scheme to the formula

$$\nu_0=T_0+v'\omega_e'-(v'^2+v')\omega_e'x_e' \tag{3.2}$$

to extract values for T_0, ω_e', and $\omega_e'x_e'$. These values were then used to predict the isotope shift between $^{56}Fe^{12}C$ and $^{54}Fe^{12}C$ for each band. The calculation of an isotope shift required an estimate for ω_e'' that we took to be $805\ \mathrm{cm}^{-1}$, the value estimated by Balfour *et al.*[8] from the observed isotope shift of a 0-0 band that was assumed to be unperturbed. The anharmonicity in the ground state was set equal to zero because no reliable estimate exists and because its contribution to the isotope shift is negligible even for a comparatively large value such as $20\ \mathrm{cm}^{-1}$. These predicted isotope shifts were then compared to the observed shifts to decide which numbering scheme was most appropriate. The results of this analysis are represented in Fig. 2. In this figure, the open circles represent the actual isotope shift as a function of $^{56}Fe^{12}C$ transition frequency, and the lines represent the calculated isotope shift for three different vibrational numbering assignments in which the first band was assigned as 1-0, 2-0, and 3-0. As the figure clearly indicates, the actual isotope shifts fall close to the line of predicted shifts for the assignment that makes the first band a 2-0 band. It was this assignment that was accepted as the true vibrational numbering of this system.

The fit of the observed bands to Eq. (3.2) with the vibrational numbering given in Table I yields $T_0=13\,167.9$

TABLE I. Spectroscopic constants[a] determined for the rotationally resolved bands of $^{56}Fe^{12}C$.

State	$v'-v''$	$\nu_0\ (\mathrm{cm}^{-1})$	$B_v'\ (\mathrm{cm}^{-1})$	$\tau\ (\mu\mathrm{s})$	$\Delta\nu_0\ (\mathrm{cm}^{-1})$[b]
$[12.0]\Omega=2$	0-0	12 045.8686(57)	0.651 788(62)	0.7600(90)	−0.1789(63)
$[13.1]^3\Phi_4$	0-0	13 063.5551(45)	0.648 961(94)	0.7140(60)	+0.5133(54)
	1-0	13 944.6164(73)	0.656 99(11)	0.5600(60)	+2.748(11)
	2-0	14 795.9545(67)	0.646 90(16)	0.4520(40)	+5.90(50)[c]
$[13.17]^3\Delta_3$	2-0	14 608.5253(45)	0.543 70(12)	7.30(20)	+4.45(50)[c]
	3-0	15 314.1551(65)	0.537 33(21)	5.00(60)	+6.63(50)[c]
	4-0	16 015.8536(56)	0.537 44(14)	6.20(10)	+9.16(50)[c]
	5-0	16 707.7139(66)	0.531 35(17)	5.70(20)	+10.89(50)[c]
	6-0	17 389.5509(59)	0.527 26(21)	6.20(20)	+12.92(50)[c]
	7-0	18 065.5348(30)	0.521 185(96)	4.10(10)	+15.23(50)[c]
$[13.18]\Omega=3$	0-0	13 175.1019(31)	0.675 270(70)	0.791(19)	+0.1108(75)
$[15.5]\Omega=3$	0-0	15 454.2026(22)	0.654 156(37)	0.7860(60)	−0.0083(63)
$[16.0]\Omega=2$	0-0	15 980.9893(38)	0.605 29(13)	2.10(20)	+1.396(11)
	1-0	16 892.7679(40)	0.597 43(13)	1.20(10)	+6.0456(95)
	2-0	17 790.5244(56)	0.585 84(15)	1.13(10)	+5.353(12)
$\Omega=2$	?-0	13 395.7831(17)	0.534 142(33)	6.73(10)	+2.3284(40)
$\Omega=2$	?-0	13 741.3114(55)	0.616 09(15)	1.15(10)	+5.2657(64)
$\Omega=2$	?-0	14 009.6807(54)	0.569 77(19)	5.91(13)	4.7502(58)
$\Omega=2$	?-0	14 393.8074(31)	0.541 603(88)	3.80(10)	+5.80(50)[c]
$\Omega=2$	?-0	14 624.7177(49)	0.574 93(19)	2.14(10)	+7.30(50)[c]
$\Omega=2$	?-0	14 972.0168(24)	0.522 741(73)	7.43(15)	+7.30(50)[c]
$\Omega=2$	?-0	16 002.7308(24)	0.542 759(53)	3.260(40)	+8.00(50)[c]

[a]The 1σ error limits in the last two decimal places for each constant are listed in parentheses following the constant. The constants ν_0 and B' were determined by fixing the lower state rotational constant to $0.669\,643\,18\ \mathrm{cm}^{-1}$ in a fit to Eq. (3.1).

[b]Unless otherwise noted, the isotope shift is the position of the band origin of the $^{54}Fe^{12}C$ species relative to that of the $^{56}Fe^{12}C$ species.

[c]This isotope shift was determined by the position of the R-band head, or other prominent feature, of the $^{54}Fe^{12}C$ species relative to the $^{56}Fe^{12}C$ species as measured from low resolution scans.

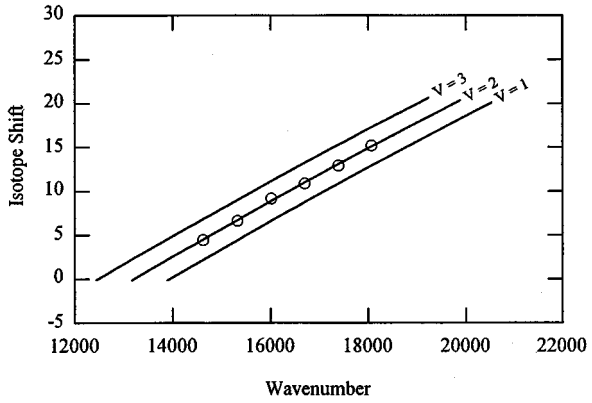

FIG. 2. Determination of the absolute vibrational numbering of the FeC $[13.17]\Omega=3$ state. The open circles represent the measured isotope shift (cm^{-1}) for each observed band in this system as a function of $^{56}Fe^{12}C$ transition energy. Using 805 cm^{-1} as an estimate for ω_e'', the predicted isotope shifts for three different vibrational assignments of the bands are plotted as continuous lines. The line marked $V=1$ corresponds to assigning the first band as 1-0; $V=2$ corresponds to 2-0; and $V=3$ corresponds to 3-0. The measured values fall on the $V=2$ line, confirming that the first band in this progression represents a transition to the $v=2$ level of the upper state.

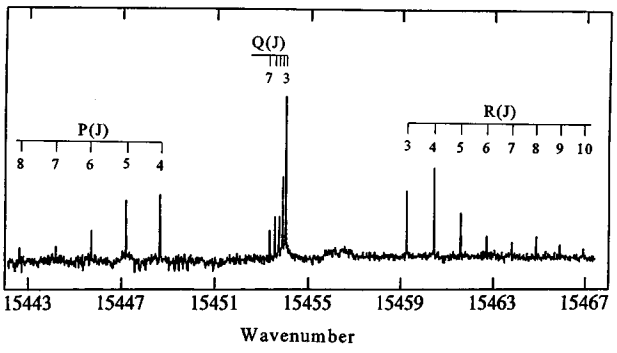

FIG. 3. Rotationally resolved spectrum of the 0-0 band of the $[15.5]\Omega=3$ state. The close spacing of the Q-branch lines indicates only a slight increase in bond length upon excitation.

± 3.6 cm^{-1}, $\omega_e'=732.2\pm 2.0$ cm^{-1}, and $\omega_e'x_e'=4.07\pm 0.19$ cm^{-1}. This assignment places the origin of this electronic state so near another $\Omega=3$ state that the traditional three digit numbering scheme for electronic states, $[xx.x]\Omega$, must be extended by one digit to uniquely identify the state. This state is therefore designated as the $[13.17]\Omega=3$ state of FeC. The values for B_v' can be extrapolated using the simple equation $B_v=B_e-\alpha_e(v+1/2)$ to determine the value of B_e to be $0.555\,45\pm 0.000\,16$ cm^{-1} and that of α_e to be $0.004\,489\pm 0.000\,029$ cm^{-1}. Finally, it is interesting to point out that the B_v' values listed in Table I decrease almost smoothly from $v'=2$ to $v'=7$ except for B_4', which is nearly the same as B_3'. It is also the 4-0 band whose isotope shift lies furthest from the $v=2$ line in Fig. 1. This indicates a perturbation in the $[13.17]\Omega=3$, $v=4$ level.

Six bands have been positively identified as belonging to this progression, but the first of these is a 2-0 band. We believe that we have located the 0-0 and 1-0 bands of this system, but their unfortunate location in the spectrum precludes any definite analysis. The 1-0 band may share its position in the spectrum with an $\Omega'=2\leftarrow\Omega''=3$ transition at about 13 890 cm^{-1}, just where it is predicted to be. The rotationally resolved spectrum of this region is quite complicated, and it was only possible to identify a few lines that might belong to the 1-0 band, so few that a good fit could not be obtained. As discussed in the next section, the 0-0 band of this system most probably lies embedded in the P branch of yet another band, again confusing the spectrum and making analysis unclear.

C. The $[13.18]\Omega=3$ and $[15.5]\Omega=3$ states

The remaining transitions with an $\Omega=3$ upper state are found at 13 175 and 15 450 cm^{-1}. Figure 3 shows the only rotationally resolved band of the $[15.5]\Omega=3$ state. As can be seen, the lines fan out symmetrically in both the P and R branches with no band head. The Q-branch lines are closely spaced and fan out to lower energy. These items indicate that the bond length increases only slightly upon excitation. The large gap between the Q and R branches, and subsequent assignment of the first rotational lines, proves that this is an $\Omega'=3\leftarrow\Omega''=3$ transition. When the spectrum is fit to Eq. (3.1) B' is found to be 0.654 156(37) cm^{-1}. It was possible to rotationally resolve the minor isotope $^{54}Fe^{12}C$ in this case, leading to an accurate determination of the isotope shift of -0.0083 ± 0.0063 cm^{-1}, very nearly zero. Such a small isotope shift indicates that this must be an origin band. This, in combination with the small change of bond length upon excitation, explains why only one vibrational level of this electronic state has been observed. Unlike the previously discussed $[13.17]\Omega=3$ state, which had a lifetime on the order of many microseconds, the lifetime of this state is about 790 ns.

The $[13.18]\Omega=3$ state possesses a rotationally resolved structure very similar to that in Fig. 3 except that the Q-branch fans out to higher energy with the lines even more narrowly spaced. This makes the $[13.18]\Omega=3$ state the only one in which the bond length is less than that in the ground state of FeC. The difference is only 0.0067 Å. This explains the lack of any other members in the progression. Again, the isotope shift is quite small, just 0.1108(75) cm^{-1}, indicating this must be a $v'=0\leftarrow v''=0$ transition. The analysis of this band posed difficulties because in the middle of the P branch appears an additional feature that could not be rotationally resolved. This feature clearly must belong to another electronic state because its measured lifetime is 7.5 times longer than the lifetime as measured in the R and Q branches where there is no evidence of anything unusual. It turns out that the position of this unresolved feature is very nearly where one would expect to find the 0-0 band for a transition to the $[13.17]\Omega=3$ state based upon the fit discussed in Sec. III B. In addition, this feature's lifetime closely matches that of the other vibrational levels of the [13.17] state. Because it was not possible to rotationally resolve the feature, its identity cannot be proven. It is also possible that what we have assigned as the $[13.18]\Omega=3$ $v=0$ level is really the

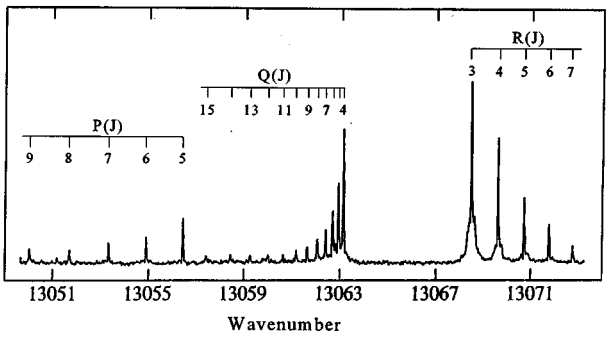

FIG. 4. Rotationally resolved spectrum of the 0-0 band of the $[13.1]\Omega=4$ state. The large gap between the branches and the relatively weak intensity of the P branch indicate an $\Omega=4\leftarrow\Omega=3$ transition that is confirmed by the fit. The entire spectrum was collected at a single excitation laser irradiance (Watts/m^2), causing the more intense R-branch lines to become power broadened.

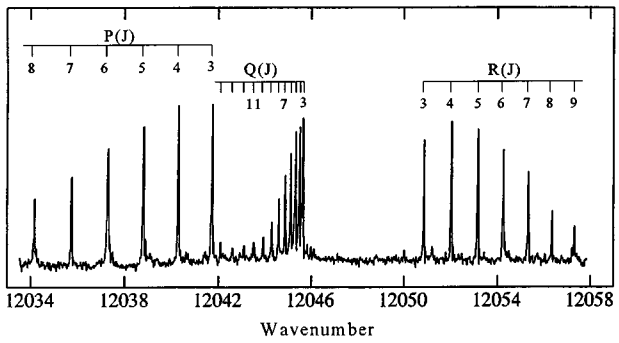

FIG. 5. Rotationally resolved spectrum of the 0-0 band of the $[12.0]\Omega=2$ state.

$[13.17]\Omega=3$ $v=0$ level, perturbed from below in such a way to give it an apparent rotational constant that is larger. If such were the case, however, it would not be expected that the lifetime as measured in the three branches would be so radically different as has been found. It would also not generally be expected that the perturbation would be so perfect as to give the fit of each line position in this band a residual less than 0.009 cm^{-1}. Because of the evidence contrary to this explanation, we feel confident that there are two different $\Omega=3$ states whose origins are near 13 175 cm^{-1}. This means that the 0-0 band of the $[13.17]\Omega=3$ is observed but not rotationally resolved.

Approximately 803 cm^{-1} to the red of the $[13.18]\Omega=3$, 0-0 band is a very weak feature that shares its distinctive rotational contour (at 0.6 cm^{-1} resolution). In low resolution, the appearance of an $\Omega'=3\leftarrow\Omega''=3$ transition that is nearly vertical with rotational constants in both states as large as 0.67 cm^{-1} is unmistakable. The Q branch is sharp and well separated from the R and P branches which fan out symmetrically on either side. The feature at 12 372 cm^{-1} may be the $[13.18]\Omega=3$, 0-1 band because of its similarity to the contour of the 0-0 band and because it is approximately 800 cm^{-1} to the red of the origin, a fact that is consistent with the value for $\Delta G''_{1/2}$ estimated by Balfour *et al.* based upon isotope shifts. The lack of a rotationally resolved scan precludes any definitive conclusion, but the observation is consistent with previous work and will have to suffice until dispersed fluorescence studies are carried out on FeC.

D. The $[13.1]\Omega=4\leftarrow X\,^3\Delta_3$ system

Only one electronic state with $\Omega=4$ was found in this study. The origin of this system is located at 13 063.5551 cm^{-1}, slightly more than 100 cm^{-1} to the red of the origin of two of the $\Omega=3$ states. The rotationally resolved scan over this band, displayed in Fig. 4, shows the large gap between the branches and the weak P branch that are characteristic of a $\Delta\Omega=+1$ transition in which Ω is large. The assignment of the first rotational lines in each branch leaves no doubt about the assignment of the electronic symmetry of the upper and lower states as $\Omega'=4$ and $\Omega''=3$. Three bands have been identified as belonging to this system based upon the trend in isotope shifts and the decreasing intensity of successive bands. The shift for the first band in the system, however, is not what would be expected for an origin band; it is too large unless the vibrational frequency increases by about 300 cm^{-1} upon excitation. This seems unreasonable and is not consistent with the values of ω'_e and $\omega'_e x'_e$ determined from the position of the band origins of each band in the progression. These values are 910.8 and 14.9 cm^{-1}, respectively. These values do properly predict the isotope shift of the second band in the progression but not the third. In addition, the B' values for each of these bands do not follow the expected pattern. There is an observed increase between the first and second bands, and the B' value for the third band is nearly the same as the first. An attempt to extract values for B_e and α_e is not very meaningful because of this problem. Despite the problems with the rotational constants and the absolute value of the isotope shifts, these three bands must belong to the same system, and we assign them as the 0-0, 1-0, and 2-0 bands. The lifetime of each of these upper states is less than a microsecond.

E. The $[12.0]\Omega=2$ electronic state

There are a number of $\Omega'=2\leftarrow\Omega''=3$ bands in the region of the current spectroscopic study, but the number of electronic states from which they derive is uncertain. There must be at least three electronic states involved to explain the observed bands. The first of these has its origin band at 12 045 cm^{-1}. The rotationally resolved spectrum of this band, the only one rotationally resolved with the OPO/OPA, is shown in Fig. 5. The assignment of the first rotational lines confirms that the lower state is again $\Omega=3$ and that Ω decreases by one unit in the transition. The isotope shift for this band is approximately -0.1 cm^{-1}. The fact that the value is negative indicates that the vibrational frequency in the upper state must be less than that in the ground state, which has been estimated to be 805 cm^{-1}. Approximately 762 cm^{-1} to the blue of this band is another whose isotope shift is 2.2 ±0.5 cm^{-1}. This band has not been rotationally resolved

because of an unfortunate spectral location, but it seems quite likely that this is the 1-0 band of this same system. The isotope shift is approximately correct, ignoring anharmonicity, and it does appear from the low resolution contour to be another $\Omega=2\leftarrow\Omega=3$ band. This provides a tentative value for $\Delta G_{1/2}$ of 762 cm^{-1}.

F. The $[16.0]\Omega=2\leftarrow X^3\Delta_3$ system

Beginning at about 15 981 cm^{-1} is a progression including three bands with $\Omega'=2$. The rotational constants for these bands follow the trend expected for three transitions that can be assigned as $(v')-0$, $(v'+1)-0$, and $(v'+2)-0$. The isotope shifts for the first two bands are not very meaningful, however. The first band has an isotope shift of 1.396(11) cm^{-1}, a number too large for a 0-0 band in this molecule. The second band has a shift of 6.0456(95) cm^{-1}, a number too large for the second member of this progression even if the shift of the first member were reasonable. If the three bands were assigned as 0-0, 1-0, and 2-0, the isotope shift for the third band is about what would be expected, 5.353(12) cm^{-1}. There is some evidence that the first of these bands is being perturbed in such a way as to give it an anomalously large isotope shift. The shift for the second band is without explanation. Despite these difficulties, a likely assignment of these bands is as 0-0, 1-0, and 2-0. The assignment is based largely upon the intensity pattern of the bands and the trend in rotational constants as well as the evidence that the first band has an isotope shift that is too large because it is perturbed. If values of ω_e' and $\omega_e'x_e'$ are extracted, the results are 925.8 and 7.0 cm^{-1}, respectively.

The evidence that the first band in this progression is perturbed deserves some explanation. First, the lifetimes of the $v=1$ and $v=2$ levels are approximately 1 μs. The $v=0$ level, however, has a lifetime of 2 μs. About 10 cm^{-1} to the blue of this band is another transition with $\Omega'=2$ that is among the ungrouped $\Omega'=2\leftarrow\Omega''=3$ transitions. This electronic state has a lifetime of slightly over 3 μs. In addition, the location of this second band for $^{54}Fe^{12}C$ is approximately 8 cm^{-1} further to the blue than that of the $^{56}Fe^{12}C$ isotope. If these two states are interacting, the interaction would be greater for the $^{56}Fe^{12}C$ isotope. Since the perturbing state is higher in energy, the origin band of the $[16.0]\Omega=2$ system would be pushed lower in energy, and to a greater extent for the major isotope, giving that band a larger than expected isotope shift. The interaction of these two states also explains the change in the lifetime: the lifetime of the $v=0$ level of the $[16.0]\Omega=2$ state is being lengthened by interaction with the state whose lifetime is longer. Presumably, the 1-0 band is being perturbed in a similar way by an unobserved state.

G. The remaining $\Omega'=2\leftarrow X^3\Delta_3$ transitions

There remain seven bands with $\Omega=2$ in the upper state cannot be assigned to any definite progressions. The band origins, rotational constants, and lifetimes determined for this set of bands are also listed in Table I under the heading of $\Omega=2$?-0 to imply that the listed bands possess $\Omega=2$ in the upper state, that their vibrational numbering is uncertain, and that they belong to an unknown number of electronic states whose origins are also unknown. All these bands do seem to originate from the ground state $v=0$ level of FeC because prior to fixing the ground state rotational constant, B'' for each band was close to 0.6696 cm^{-1}. Despite the fact that we have been unsuccessful in grouping these bands by electronic state, they do share properties in common. First, they all possess long lifetimes, all greater than a microsecond and some considerably longer than that. Each also has an isotope shift greater than 2 cm^{-1}, a number too large to make any of these bands likely candidates for an origin band. For the most part, their upper state rotational constants indicate that upon excitation the bond length increases significantly, in much the same manner as that observed in the $[13.17]\Omega=3$ electronic state. Other than these general features, very little can be said about these bands.

H. Ionization energy of FeC

To the red of the origin band of the $[12.0]\Omega=2$ system near 12 040 cm^{-1}, the intensity of transitions steadily falls until, finally, below 11 700 cm^{-1} no new transitions are observed. Given that the rest of the observed spectrum has a number of transitions every few hundred wavenumbers, it was reasoned that observing new transitions below 12 000 cm^{-1} might be impossible because there was no longer sufficient energy to ionize FeC in a two photon process. It is also possible, however, that no spectroscopically accessible states exist below 12 000 cm^{-1}. To test this notion, the output of the excimer used for photoionization was Raman shifted to provide the first Stokes radiation at an energy 4155 cm^{-1} lower than the ArF laser output. An attempt was made to scan the spectrum of FeC again with this lower energy photon for ionization to look for an ionization threshold in a region that did have known electronic transitions. The signal to noise ratio was too low, however, for any distinct and reproducible features to be observed. Instead, it was possible to compare the signal obtained from attempting to ionize a single vibronic transition with the ArF excimer laser output to that obtained with the Raman shifted excimer laser output after summing 100 experimental cycles. This provided a much better signal to noise ratio and allowed an ionization threshold to be determined.

The results of this experiment are shown in Fig. 6. This figure consists of four mass spectra showing iron atom to the left in each pane and iron carbide at mass 68 amu. Each mass spectrum was collected at a different total energy available for ionization, and each is plotted on the same vertical scale for comparison. Part (a) of this figure illustrates that resonant enhancement at the mass of $^{56}Fe^{12}C$ is clearly seen when attempting to ionize the $v=1$ level of the $\Omega=4$ state near 13 950 cm^{-1} with the ArF excimer laser output. Part (b) shows that the enhancement disappears when ionization of the same state is attempted with Raman shifted ArF excimer radiation. Clearly, the energy available in (b) is not sufficient to ionize the molecule. Part (c) shows the enhancement found when ionizing the $v=0$ level of the $\Omega=3$ state near 15 450 cm^{-1} with ArF excimer radiation. Changing to Ra-

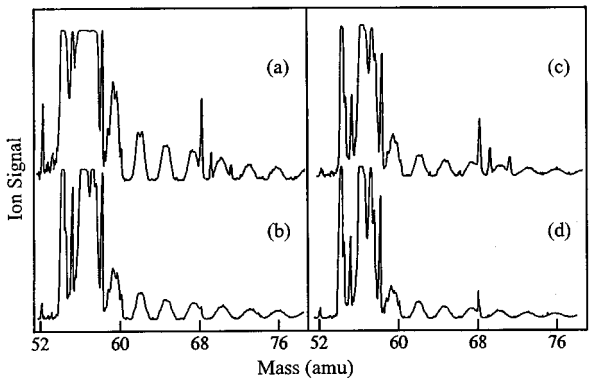

FIG. 6. Determination of the ionization energy of FeC. Four mass spectra are displayed, each taken at a different total energy available for ionization. Atomic iron is the largest signal in each spectrum at the left, and $^{56}Fe^{12}C$ is at mass 68 amu. The total energy available is just the sum of the energies of the excitation photon and the ionization photon. In the four panes, these energies are (a) 14 394 cm^{-1}+6.42 eV, (b) 14 394 cm^{-1}+5.90 eV, (c) 15 454 cm^{-1}+6.42 eV, (d) 15 454 cm^{-1}+5.90 eV. When going from (a) to (b) the transition being probed is no longer observed as the ionization photon energy is decreased. This does not happen on going from (c) to (d); therefore, the total energy available in (b) and (d) brackets the IE as 7.74 ±0.09 eV.

man shifted ArF radiation for ionization in part (d) does decrease the intensity of the enhancement, but it does not eliminate it, indicating that there is sufficient energy available for ionization. A number of other bands between the two illustrated in Fig. 6 were probed in a similar fashion, and none showed any enhancement when ionization was attempted with a Raman shifted ArF excimer. When ionized with the pure ArF excimer, however, these bands showed less ion enhancement than that observed in Fig. 6(c), making a definitive determination of when ion enhancement disappeared upon switching to Raman shifted ArF radiation for ionization quite difficult and somewhat subjective. The choice of the bands at 15 450 and 13 950 cm^{-1} to bracket the IE of FeC then represents a conservative range in which we are confident the ionization energy of FeC truly falls.

Assuming that the transitions excited in Figs. 6(b) and 6(d) originate from the ground state of the molecule and that there are no Frank–Condon difficulties in the ionization step, the ionization threshold for FeC can be narrowed to the region between the 13 950 and 15 450 cm^{-1} bands when 5.905±0.004 eV radiation is used for ionization. To determine the ionization energy (IE) of the molecule, the known band origins of these two transitions were averaged, added to the energy of the Stokes-shifted ArF radiation, and this value was then corrected for the effect of field ionization due to the static electric field present in the extraction region of the TOFMS. The correction amounted to 0.013 94 eV in the 337.5 V/cm electric field used. The error associated with this IE is simply half the difference between the origins of the two bands used to bracket the IE, giving a final value of IE(FeC)=7.74±0.09 eV.

IV. DISCUSSION

A. The electronic state manifold of FeC

Every rotationally resolved band in this study of iron monocarbide originates from an $\Omega=3$ state. This confirms that the ground state possesses an Ω of 3, probably originating from an inverted $^3\Delta$ term. The previous study by Balfour *et al.* provided the first spectroscopic identification of FeC in the gas phase and identified two excited electronic states, both of $\Omega=3$ symmetry, the positions of which could be determined relative to the ground state. Other electronic states were observed in that study, but placing them on the same energy scale is impossible because no spectroscopic transitions connected them to the ground state. The current study adds six new electronic states to this picture that can be located relative to the ground state. Three of these states have $\Omega=3$, one has $\Omega=4$, and two possess $\Omega=2$. There must be at least one more $\Omega=2$ state (most likely more than one), but we are uncertain of its origin because of extensive perturbations. A summary of the known information about the electronic states that can be located relative to the ground state is listed in Table II.

TABLE II. Spectroscopic constants[a] for the known electronic states of $^{56}Fe^{12}C$.

State	T_0 (cm^{-1})	ω_e (cm^{-1})	$\omega_e x_e$ (cm^{-1})	B_e (cm^{-1})	α_e (cm^{-1})	r_e (Å)
$[20.3]\Omega=3$[b]	20 273.60(5)[b]	$\omega_e\sim730$[b]		$B_0=0.5813(5)$[b]		$r_0=1.7132(7)$[b]
$[20.2]\Omega=3$[b]	$\sim$20,199[b,c]	$\Delta G_{5/2}=671.80(7)$[b]		$B_2=0.5321(5)$[b]		$r_2=1.7907(8)$[b]
$[16.0]\Omega=2$	15 980.9893(38)	925.8[d]	7.0[d]	$B_0=0.605\ 29(13)$		$r_0=1.678\ 92(17)$
$[15.5]\Omega=3$	15 454.2026(22)	⋯		$B_0=0.654\ 156(37)$		$r_0=1.614\ 998(46)$
$[13.18]\Omega=3$	13 175.1019(31)	⋯		$B_0=0.675\ 270(70)$		$r_0=1.589\ 549(82)$
$[13.17]^3\Delta_3$	13 168(4)	732(2)	4.1(2)	0.555 45(16)	0.004 489(29)	1.752 64(26)
$[13.1]^3\Phi_4$	13 063.5551(45)	910.8[d]	14.9[d]	$B_0=0.648\ 961(94)$		$r_0=1.621\ 45(12)$
$[12.0]\Omega=2$	12 045.8686(57)	$\Delta G_{1/2}=762(1)$		$B_0=0.651\ 788(62)$		$r_0=1.617\ 929(77)$
$X^3\Delta_3$	0.00	$\Delta G_{1/2}\sim804$[e]		$B_0=0.669\ 643\ 18(7)$[f]		$r_0=1.596\ 213\ 4(1)$[f]

[a]Constants are reported with a 1σ error estimate in parentheses. Except where specifically indicated, all data is from the current work.
[b]This data was taken from the laser induced fluorescence work by Balfour *et al.* on FeC. See Ref. 8.
[c]Estimated assuming $\omega_e' x_e'=0$ for this state and assuming that the two observed vibrational levels are not perturbed.
[d]Because only three band origins were used to determine both ω_e' and $\omega_e' x_e'$, the values reported here are unique and have no meaningful error bar associated with them from the fit.
[e]This value is based on an estimate by Balfour *et al.* from isotope shifts and a tentative assignment of a hot band in this study. See Ref. 8.
[f]This value was determined by the millimeter wave study of the ground state by Allen and co-workers in Ref. 23.

Making sense of the electronic states observed in FeC is facilitated by a rudimentary molecular orbital analysis. The best point of reference for such a discussion is CoC,[9] a molecule for which a great deal is known about the character of the molecular orbitals involved in the bonding because of extensive hyperfine analyses of the observed bands. In comparison to the $3d$ transition metal oxides, it is generally true that there will be a better energy match between the atomic orbitals of carbon and those of the metal because of the lower ionization energy of atomic carbon as compared to atomic oxygen. The resultant increase in the interaction between these atomic orbitals in the formation of molecular orbitals is at least one of the reasons CoC, a molecule that is isovalent to MnO, does not possess a $^6\Sigma^+$ ground state as does MnO.[6] In the carbides, the bonding 8σ and 3π orbitals are pushed lower in energy by this interaction and the corresponding antibonding orbitals are pushed higher, making the loss of exchange energy upon pairing electrons in the 1δ and 9σ orbitals less unfavorable and allowing the $^2\Sigma^+$ term arising from a $8\sigma^2 3\pi^4 1\delta^4 9\sigma^1$ configuration to emerge as the ground state of CoC. If, at this point, a molecular orbital diagram would be useful in understanding these configurations, the reader is referred to one of the several MO diagrams that have been published that can be considered relevant to FeC.[8–10] Perhaps the most useful is that presented by Adam and Peers in their work on CoC.[10]

In the case of CoC, it was shown that the character of the 9σ orbital was largely metal $4s$ (89%) with the remainder most likely made up of metal $3d_\sigma$. From analysis of an excited $^2\Delta$ state deriving from a $1\delta^3 9\sigma^2$ configuration, it was possible to determine the character of the 1δ orbital. As expected, it is primarily metal $3d$ in character (86%). As such, both of these orbitals are mainly nonbonding. The more important observation, however, was that the states derived, from these two electron configurations are only separated by a few hundred wavenumbers. The $^2\Delta_{5/2}$ component lies just 221 cm^{-1} above the ground state. To the extent that the molecular orbital picture can be believed, the two electron configurations considered here are very nearly degenerate. Stretching the point even further, the two molecular orbitals 1δ and 9σ can be considered to lie very close in energy with the 1δ slightly lower.

On moving from CoC to FeC, one would not expect dramatic changes to take place in the nature of the bonding. The ionization energies of Fe and Co are similar enough that the degree of interaction of the atomic orbitals on the metal and carbon atoms can be considered to be about the same. The metal d orbitals will certainly be raised slightly in energy, possibly bringing the 1δ orbital even closer to the 9σ. The electron that is removed on going from CoC to FeC is one of the 1δ electrons. Because the 1δ and 9σ orbitals are so nearly degenerate, not enough energy can be gained by forming a $1\delta^4$ configuration to recoup the loss of exchange energy. Such an argument at least serves to rationalize why the ground state of FeC should be $^3\Delta_i$ deriving from a $8\sigma^2 3\pi^4 1\delta^3 9\sigma^1$ configuration.

In the work on CoC by Adam and Peers, the observed excited state was a $^2\Sigma^+$ with a bond length that was greater than the ground state's by about 15%.[10] There it was argued that this must correspond to a charge transfer transition in which an electron mainly localized on the carbon atom is being moved to a molecular orbital that is mainly localized on the metal center. Such a conclusion was justified by the results of the hyperfine analysis. Based on this analysis, the only reasonable configuration for the $[14.0]^2\Sigma^+$ state was $8\sigma^1 3\pi^4 1\delta^4 9\sigma^2$. In the case of FeC, the $[13.17]\Omega=3$ electronic state has its origin only about 800 cm^{-1} to the red of this transition in CoC. In addition, the bond length change in this transition is considerable. It increases by about 11% when comparing the r_0 values for the two states. Such an increase is consistent with what would be expected for a charge transfer transition. Based on the similarities between the $[14.0]^2\Sigma^+$ state of CoC and the $[13.17]\Omega=3$ state of FeC, we assign the $[13.17]\Omega=3$ state of FeC as a $^3\Delta_3$ state deriving from the $8\sigma^1 3\pi^4 1\delta^3 9\sigma^2$ molecular configuration. Both the $[14.0]^2\Sigma^+ \leftarrow X^2\Sigma^+$ system of CoC and the $[13.17]^3\Delta_3 \leftarrow X^3\Delta_3$ system of FeC then correspond to a $9\sigma \leftarrow 8\sigma$ electronic excitation.

Definite molecular orbital assignments for the remainder of the observed electronic states are more troublesome to make. If it is assumed that the selection rules of $\Delta\Lambda = \pm 1,0$ and $\Delta\Sigma = 0$ are in force in this molecule, the $[13.1]\Omega=4$ state observed in this study must certainly be the $\Omega=4$ component of a $^3\Phi$ state. Several configurations can generate this term. The lowest of these in energy are $8\sigma^2 3\pi^4 1\delta^3 9\sigma^0 4\pi^1$, $8\sigma^2 3\pi^4 1\delta^2 9\sigma^1 4\pi^1$, and $8\sigma^2 3\pi^3 1\delta^3 9\sigma^2$. It is impossible to say exactly which is responsible for the $^3\Phi$ state. The last of these might be considered the least likely because it, like that of the configuration identified as giving rise to the $[13.17]^3\Delta_3$ state, represents a charge transfer transition from the ground state. The $[13.1]\Omega=4$ state is not accompanied by such a large change in bond length upon excitation, however, and therefore is not consistent with a charge transfer transition. Under the same selection rules, this last configuration may be able to account for the observation of at least one $\Omega=2$ state because some of the observed $\Omega=2$ states that could not be grouped by electronic state possess bond lengths that are considerably longer than that of the ground state.

The other two configurations listed above, $8\sigma^2 3\pi^4 1\delta^3 9\sigma^0 4\pi^1$ and $8\sigma^2 3\pi^4 1\delta^2 9\sigma^1 4\pi^1$ can also generate $^3\Pi$ states that can give rise to other $\Omega=2$ states, and they undoubtedly play a role in some of the transitions observed here. It is difficult to find enough $^3\Delta$ terms from simple one electron excitations to account for all the $\Omega=3$ states observed in this study and in Balfour's study. Some of the observed $\Omega=3$ states may derive from two electron transitions, indicating that the single configuration approximation is invalid. In any case, the simple molecular orbital picture does not suffice to entirely explain the complete electronic state manifold of FeC, but it does explain some of its important features.

B. Bond strength of FeC

The ionization energy determined for FeC is less than that of atomic iron (7.9024 eV)[24] by 1310 ± 726 cm^{-1}. This

indicates that the ground state of FeC is very nearly as strongly bound as the ground state of the cationic species. In the case of FeC, it is possible to make this comparison more quantitative because the bond strength of FeC^+ has been determined. Hettich and Freiser[25] have studied the photodissociation behavior of $FeCH_2^+$ as a function of wavelength and have determined that $D_0(FeC^+)=4.1\pm0.3$ eV. It is questionable whether the value determined by Hettich and Freiser is truly the dissociation energy due to the rather low density of electronic states in $FeCH_2^+$, but this value does, at any rate, represent an upper limit. The dissociation energy of the ground state neutral can then be determined by the value of $IE(FeC)+D_0(FeC^+)-IE(Fe)$. This gives a value for $D_0(FeC)$ of 3.9 ± 0.3 eV, where the error is dominated by the uncertainty in the value of $D_0(FeC^+)$. Again, this represents an upper limit to the bond strength of the neutral.

The similarity of the derived neutral FeC bond strength to that of the cationic species FeC^+ is reassuring. The neutral possesses a single unpaired electron in the 9σ orbital, which was shown to be largely metal $4s$ in character by both of the studies of CoC. Some of the remaining character of this orbital is probably metal $3d_\sigma$ and metal $4p$, allowing the 9σ orbital to polarize away from the negatively charged carbon atom. The ground state of the cation is presumably $^2\Delta$, meaning that it is the lone 9σ electron that is removed in the ionization step. This makes sense because the metal's valence d orbitals, which are largely responsible for the molecular δ orbital, certainly lie below the metal's valence s orbital by the time we have reached Fe in the $3d$ series. Removal of the mainly nonbonding 9σ electron upon ionization leads one to expect only a slight change in the bond energy as is observed. One might expect $D_0(FeC^+)$ to be slightly larger than $D_0(FeC)$ because of the added Coulombic interaction, but the error bars on the values are too large to be definitive on this point. A less circuitous route to the same conclusion is to compare the ionization energies of FeC and atomic iron. They are so similar because the electron being removed to form the ion FeC^+ is mainly an Fe $4s$ electron.

V. CONCLUSION

This investigation of FeC has increased the information available about the excited electronic states of the first $3d$ transition metal carbide to be identified in the gas phase by its electronic spectrum. Six electronic states, consisting of 15 rotationally resolved bands, have been positively positioned relative to the ground state. The remainder of the observed transitions all are $\Omega=2\leftarrow\Omega=3$ type transitions, but it has proven impossible at this point to group them into electronic systems. One of the $\Omega=3$ states can be ascribed to a charge transfer transition in which one of the 8σ electrons, mainly localized on the carbon atom, is promoted to the 9σ, an orbital that is mainly metal $4s$ in character. This conclusion is supported by the large increase in bond length upon excitation. If this assignment is correct, the transition is the analog of the $[14.0]^2\Sigma^+\leftarrow X^2\Sigma^+$ transition in CoC that has been identified as a charge transfer system. The ionization energy of FeC has been determined to be 7.74 ± 0.09 eV, leading to a calculation of $D_0(FeC)$ as 3.9 ± 0.3 eV.

ACKNOWLEDGMENTS

We thank the U.S. Department of Energy (DE-FG03-93ER143368) for support of this research. We also acknowledge the donors of the Petroleum Research Fund, administered by the American Chemical Society, for partial support of this research. The University of Utah is also acknowledged for its partial support of this work in the form of a fellowship for D.J.B.

[1] O. Appelblad, R. F. Barrow, and R. Scullman, Proc. Phys. Soc. **91**, 261 (1967).
[2] B. Kaving and R. Scullman, J. Mol. Spectrosc. **32**, 475 (1969).
[3] K. Jansson and R. Scullman, J. Mol. Spectrosc. **36**, 268 (1970).
[4] R. Scullman and B. Thelin, Phys. Scr. **5**, 201 (1972).
[5] B. Simard, P. A. Hackett, and W. J. Balfour, Chem. Phys. Lett. **230**, 103 (1994).
[6] A. J. Merer Annu. Rev. Phys. Chem. **40**, 407 (1989).
[7] I. Shim, M. Pelino, and K. A. Gingerich, J. Chem. Phys. **97**, 9240 (1992).
[8] W. J. Balfour, J. Cao, C. V. V. Prasad, and C. X. W. Qian, J. Chem. Phys. **103**, 4046 (1995).
[9] M. Barnes, A. J. Merer, and G. F. Metha, J. Chem. Phys. **103**, 8360 (1995).
[10] A. G. Adam and J. R. D. Peers, J. Mol. Spectrosc. **181**, 24 (1997).
[11] We have collected a low resolution spectrum for TiC. A few bands have been rotationally resolved but not successfully analyzed. We have also collected a low resolution spectrum of VC without any luck in rotationally resolving the observed bands. In addition, two vibronic transitions in CrC have been observed, and one has been rotationally resolved. Analysis is pending. We have also collected an extensive spectrum of NiC and rotationally resolved 30 of the observed bands, work that will be published soon.
[12] Z. Fu, G. W. Lemire, Y. M. Hamrick, S. Taylor, J.-C. Shui, and M. D. Morse, J. Chem. Phys. **88**, 3524 (1988).
[13] S. C. O'Brien, Y. Liu, Q. Zhang, J. R. Heath, F. K. Tittel, R. F. Curl and R. E. Smalley, J. Chem. Phys. **84**, 4074 (1986).
[14] G. W. Lemire, G. A. Bishea, S. A. Heidecke, and M. D. Morse, J. Chem. Phys. **92**, 121 (1990).
[15] M. Barnes, P. G. Hajigeorgiou, R. Kasrai, A. J. Merer, and G. F. Metha, J. Am. Chem. Soc. **117**, 2096 (1995).
[16] D. J. Clouthier and J. Karolczak, Rev. Sci. Instrum. **61**, 1607 (1990).
[17] J. M. Behm, D. J. Brugh, and M. D. Morse, J. Chem. Phys. **101**, 6487 (1994).
[18] P. R. Bevington, *Data Reduction and Error Analysis for the Physical Sciences* (McGraw Hill, New York, 1969). The CURFIT program beginning on p. 237 was used as the core of the nonlinear least squares routine used to fit lifetime decay curves.
[19] S. Gerstenkorn and P. Luc, *Atlas du Spectre d'Absorption de la Molécule d'Iode entre 14,800–20,000 cm^{-1}* (CNRS, Paris, 1978).
[20] S. Gerstenkorn, J. Verges, and J. Chevillard, *Atlas du Spectre d'Absorption de la Molécule d'Iode entre 11,000–14,000 cm^{-1}* (CNRS, Paris, 1982).
[21] S. Gerstenkorn and P. Luc, Rev. Phys. Appl. **14**, 791 (1979).
[22] See AIP Document No: PAPS JCPSA-107-9772-22 for 22 pages of absolute line positions. Order by PAPS number and journal reference from American Institute of Physics, Physics Auxiliary Publication Service, Carolyn Gehlbach, 500 Sunnyside Boulevard, Woodbury, NY 11797-2999. Fax: 516-576-2223, Electronic mail: paps@aip.org. The price is $1.50 for each microfiche (48 pages) or $5.00 for photocopies up to 30 pages, and $0.15 for each additional page over 30 pages. Airmail additional. Make checks payable to the American Institute of Physics.
[23] M. D. Allen, T. C. Pesch, and L. M. Ziurys, Ap. J. **472**, L57 (1996).
[24] E. F. Worden, B. Comaskey, J. Densberger, J. Christensen, J. M. McAfee, and J. A. Paisner, J. Opt. Soc. Am. B **1**, 314 (1984).
[25] R. L. Hettich and B. S. Freiser, J. Am. Chem. Soc. **108**, 2537 (1986).